

Diblock Copolymers: Comicellization and Coadsorption

D. F. K. Shim,* C. Marques,† and M. E. Cates

*Theory of Condensed Matter Group, Cavendish Laboratory, Madingley Road, Cambridge CB3 0HE, U.K.**Received February 5, 1991; Revised Manuscript Received May 7, 1991*

ABSTRACT: In this paper we study the conditions under which comicellization occurs for a bimodal distribution of diblock copolymers in a selective solvent. The formation of pure micelles or comicelles depends on the relative concentration of the two species of diblock copolymers in solution. Regions of pure micelles in equilibrium with the free chains belonging to the two species exist in the phase diagram at low concentrations of one or other species, but for high enough concentrations of both species, comicelles may be present depending on the interaction parameter of the bimodal core. We consider the effects of varying this interaction parameter. We also discuss the interfacial behavior of mixed copolymer systems, and the conditions under which monodisperse or bimodal "brushes" of adsorbed polymer will form on an attractive surface.

I. Introduction

The macromolecular analogues of micelle-forming surfactants, amphiphilic diblock copolymers AC in a selective solvent, have been extensively studied.¹⁻⁹ Various theoretical models have been put forward to gain a better understanding of these micelle-forming diblock copolymers and have been used to explain some of the experimental observations.¹⁰

We consider the case of a highly selective solvent in which one of the blocks, say A, is incompatible with the solvent and with the C block and forms a near-molten core, excluding most of the solvent and the C polymer. The other block C solubilizes preferentially in the solvent and forms a "corona" fanning outward from the core. This region is analogous to a set of terminally attached polymers on the molten core/corona interface.

The asymmetry of the diblock copolymer is characterized by the parameter $\beta_{AC} = N_C^{3/5} N_A^{-1/3}$. This is simply the ratio of the sizes in the solvent of the two blocks making up the diblock copolymer. (We assume that the statistical lengths of A and C species are equal and choose units so that this length $l = 1$.) In most practical cases where the diblock copolymer is in selective solvent, $\beta \neq 1$.

Diblock copolymers are also used to study the physical properties of polymer-coated particles.¹¹ They impart stability on colloidal particles and prevent the particles from coagulating or flocculating in a dispersion. The block that has a high affinity for the surface and interacts unfavorably with the solvent precipitates onto the colloid surface and the block that has a lower surface affinity then forms the solvated corona, which acts as a stabilizing layer. If the thickness of the solvated layer is much smaller than the radius of the colloidal particle, then the stabilizing layer can be modeled as a grafted layer on a flat surface. This has been extensively studied by many authors.¹²⁻¹⁹ This approximation is not unreasonable and provides the route for calculating the interaction between colloidal particles.¹¹

These two problems—formation of micelles and adsorption—have been previously addressed by Marques et al.¹ who assumed a monodisperse distribution of diblock copolymer chains in solution. In many experimental situations it is of some interest to modulate the micelles

and adsorbed layer characteristics—for instance, the micelle aggregation number or the thickness of the adsorbed layer—by mixing molecules of different types.

In this paper we present an extension of the model of ref 1 to a bimodal distribution of diblock copolymers. We consider two species of diblock copolymers AC and BC with asymmetry parameter β_{AC} and β_{BC} , respectively. Their degrees of polymerization (DP) are $(N_A + N_1)$ and $(N_B + N_2)$, respectively. For simplicity we restrict our attention to the case $N_A = N_B = N$. Both A and B are in bad solvent and hence in a collapsed state, while for C the solvent is good; each C block forms a dangling tail attached to a molten head of A or B. The objectives of this paper are to consider situations under which composite micelles ("comicelles") can arise from the two different species. This represents the simplest case of a more general problem involving the statistics of micelle formation from a distribution of diblock copolymers in a selective solvent. There is a close analogy with the theory of competitive adsorption by different species and we will consider this problem within the same framework. Diblock copolymers make good theoretical models for studying micellization (even though their critical micellization concentrations are small). This is because polymeric interactions and free energies are more universal and better understood than the forces between smaller molecules. Strictly speaking our results apply only for asymptotically long chains, but many of the qualitative aspects should hold for short chains also. With this in mind, we deliberately use rather small values of the DP when illustrating our results with numerical phase diagrams.

The paper is organized as follows. In section II we present the theory of comicellization. We determine the grand canonical free energy of a comicelle in equilibrium with its unassociated bulk components. We show how comicelles can form for three different cases; χ_{AB} negative, zero, and slightly positive. Here χ_{AB} is the usual Flory interaction parameter between the A and B chains. We present our results in the form of a schematic phase diagram showing concentration regimes where comicelles and/or pure micelles arise. In section III we formulate the problem of coadsorption when the two species are in the presence of an attractive wall. The results are again summarized on a schematic phase diagram. In section IV we present possible variations to the problem below and summarize the results of section II and III on a combined schematic phase diagram plot.

* To whom correspondence should be addressed.

† Present address: Institut Charles Sadron, 6, rue Boussingault, 67083 Strasbourg Cedex, France.

II. Theory

II.1. Comicellization. At extremely low bulk chain concentrations c_1 and c_2 of the two species AC and BC, referred to as type 1 and type 2 henceforth, the diblock copolymers do not aggregate and the chains behave independently of each other. Each of the two species has an insoluble block A or B with DP N , attached to a C block of DP N_1 or N_2 , respectively, for which the solvent is good. In this section we restrict ourselves to $\beta_{BC} > \beta_{AC} > 1$; this requires $N_2 > N_1 \gg N$. For simplicity we also assume below that the interfacial tension with the solvent is the same for A and B. Clearly for different A and B, this constraint may seem somewhat unrealistic but nevertheless provides an insight into the process of micellization/comicellization where the interfacial tensions are a significant component in their behavior. Different surface tensions can easily be incorporated into the theory for more detail study of particular systems.

We construct below the grand canonical free energy Ω of a comicelle in equilibrium with the bulk species 1 and 2. The comicelle is made up of $p = p_1 + p_2$ chains with p_1 chains of type 1 and p_2 of type 2 (see Figure 1). We can think of the comicelle as follows. If we consider the core and the inner corona only we can imagine this as a micelle consisting of p chains with the core radius³ $R_m \sim (pN)^{1/3}$ and the corona size $R_1 \sim p^{1/5}N_1^{3/5}$. We then consider this as a new "core" and add a second outer corona with width $R_2 \sim (p_2^{1/3}\Delta N + p^{1/3}N_1)^{3/5} - p^{1/5}N_1^{3/5}$, where $\Delta N = (N_2 - N_1)$. We can now write the grand canonical free energy as

$$\Omega(p, p_2) = F_\gamma + F_{\text{corona}} + F_{\text{core}} - \mu_1 p - \Delta\mu p_2 \quad (1)$$

where $\Delta\mu = \mu_2 - \mu_1$.

The first term F_γ is the effective interfacial energy between the molten core of the comicelle and the solvent, which has the form

$$F_\gamma = \gamma_{\text{eff}} N^{2/3} p^{2/3} \quad (2a)$$

where γ_{eff} is the effective interfacial tension between the core surface and the solvent calculated below.

The corona energy F_{corona} consists of two terms, one of the inner corona and the other of the outer corona. They have the form

$$F_{\text{corona}} = a(p)p^{3/2} + b(p, p_2)p_2^{3/2} \quad (2b)$$

where

$$a(p) = \log(N^{-1/3}p^{-2/15}N_1^{3/5})$$

and

$$b(p, p_2) = \log\left[\frac{(p_2^{1/3}\Delta N + p^{1/3}N_1)^{3/5}}{p^{1/5}N_1^{3/5}}\right]$$

This form for the corona energy is derived from the Daoud and Cotton model for star polymers.³

The mean-field interaction energy between the species in the bimodal core is given by

$$F_{\text{core}} = \chi_{AB}N(p - p_2)p_2/p \quad (2c)$$

Finally μ_1 and μ_2 are respectively the chemical potential of unassociated type 1 and 2 chains in the bulk. Assuming as usual that the translational entropy of the aggregates is negligible¹ compared to that of unassociated species, these are given for $i = 1, 2$ as

$$\mu_i = \log c_i + \Delta F_i \quad (3)$$

The first term is the usual translational entropy term where

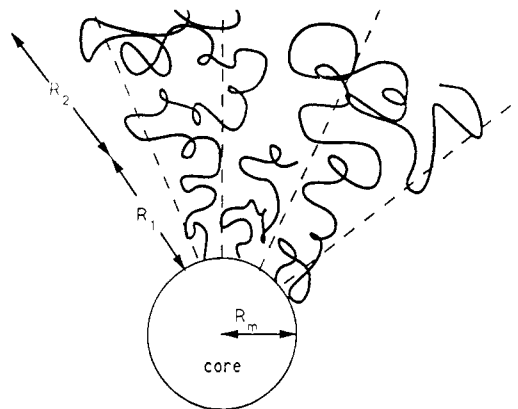


Figure 1. Spherical comicelle made up of two species of diblock copolymer, one short and the other long.

c_i is the concentration of unassociated chains of type i . (Here and below, we work in units where $k_B T = 1$ and assume the size of a monomer unit $a = 1$ for all three chain species.) To avoid an unphysical self-energy term, we have introduced ΔF_i as the extrapolation to $p = p_i = 1$ of the free energy estimated above for a pure micelle containing p_i chains. This gives

$$\Delta F_1 = 4\pi\gamma_{AO}r^2 + \log(N^{-1/3}N_1^{3/5}) \quad (4a)$$

and

$$\Delta F_2 = 4\pi\gamma_{BO}r^2 + \log(N^{-1/3}N_2^{3/5}) \quad (4b)$$

where $r = (3/4\pi)^{1/3}N^{1/3}$ is the radius of the molten head of an unassociated diblock copolymer and γ_{AO} and γ_{BO} are the interfacial tension between the polymers A and B and the solvent (O), respectively. For simplicity of calculations we set $(36\pi)^{1/3}\gamma_{AO} = (36\pi)^{1/3}\gamma_{BO} = \gamma_{\text{eff}}$ (see eq 2a). The first term of eqs 4a and 4b is the surface energy of the collapsed head of the diblock copolymer. The second terms are excluded-volume self-energies and are small compared to the interfacial terms, which are of order $N^{2/3}$. These terms ensure that on extrapolation to small aggregation numbers we arrive at $\Omega(p=1, p_2=0) \sim -\log c_1$ and $\Omega(p=p_2, p_2=1) \sim -\log c_2$ as required on the basis of our assumption that the micelles/comicelles in solution have negligible translational entropy.

In this construction we have neglected the elastic energy contribution of the micelle core, which is always very small. As appropriate near the micellization threshold, we assume a dilute solution of diblock copolymers and so neglect the exterior osmotic pressure acting on the coronas.¹ Another neglected term consists of the entropic contribution due to mixing of the junction points at the interface of the micelle. We have found in general that adding this contribution shifts only slightly the equilibrium values of p_1 and p_2 and their respective comicellization chemical potentials. An exception is in the range where we predict pure micelles of one species, in which case the entropy of mixing term ensures that an exponentially small proportion of the micelles will contain a chain of the other type. With this provision, we neglect this term in what follows. (Likewise, neglect of the translational entropy of micellized species means that we predict no dispersion in aggregation numbers.) This also allows for more direct comparison with the calculations of ref 1 for the case of a single species.

Minimization of eq 1 with respect to p and p_2 leads to

$$\mu_1 = \frac{\partial}{\partial p}(F_\gamma + F_{\text{corona}} + F_{\text{core}}) \quad (5)$$

and

$$\Delta\mu = \frac{\partial}{\partial p_2}(F_\gamma + F_{\text{corona}} + F_{\text{core}}) \quad (6)$$

respectively.

Critical comicellization occurs when we have $\Omega \approx 0$ giving

$$\frac{1}{3}\gamma_{\text{eff}}N^{2/3}p^{2/3} + \left[\frac{2}{15} - \frac{a(p)}{2} \right] p^{3/2} = \frac{1}{2}b(p,p_2)p_2^{3/2} \quad (7)$$

after eliminating μ_1 and $\Delta\mu$ using eqs 5 and 6.

We note from eq 7 that for a given aggregation number p , the relative amounts of each species $p_1(p)$ and $p_2(p)$ are independent of the interaction parameter χ_{AB} between the A and B blocks. Instead the role of χ_{AB} is to alter the value of p at which comicellization occurs, as we shall see below. To study the comicellization process we may attempt the following. Suppose initially we start with a solution of unassociated type 1 and 2 species in bulk solution such that the ratio of their total volume fraction Φ_1 and Φ_2 is given by $K = \Phi_2/\Phi_1$. We now increase the volume fraction of types 1 and 2, while keeping K constant until micellization or comicellization occurs. Repeating this process for different values of K , we can build up a phase diagram separating regions of unassociated chains, monodisperse micelles with free chains, and comicelles with free chains. We will refer to the two chain concentrations at which comicellization occurs as the critical comicellization concentrations (ccc), which are simply related to the total volume fraction at comicellization by $\Phi_i^{\text{ccc}} = N_i c_i^{\text{ccc}}$. The locus of these points on the phase diagram defines the comicellization boundary. Similarly we have the micellization boundary, which separate regions of free chains and monodisperse micelles with unassociated chains. In these regions only one of the type attains its cmc. We also define *mixing lines* as the lines in the phase diagram separating regions of monodisperse micelles in equilibrium with free chains from comicelles in equilibrium with free chains. In particular we will study the effect of varying χ_{AB} on the comicellization boundary.

To study quantitatively the evolution of p_1 and p_2 along the comicellization boundary, we may envisage the following. We begin with pure solution of type 1 with Φ_1 just above Φ_1^{cmc} . The micellization for this solution occurs for $\mu_1 = \mu_1^{\text{cmc}}$, where μ_1^{cmc} is given by

$$\mu_1^{\text{cmc}} = (p_1^{\text{cmc}})^{1/2} \left[\frac{5a(p_1^{\text{cmc}})}{2} - \frac{2}{5} \right] \quad (8)$$

and p_1^{cmc} is the equilibrium number of chains in the micelle given by the solution to the equation below

$$\frac{1}{3}\gamma_{\text{eff}}N^{2/3}p_1^{2/3} = \left[\frac{a(p_1)}{2} - \frac{2}{15} \right] p_1^{3/2} \quad (9)$$

Both eqs 8 and 9 are derivable from the model of eq 1.

Next we add species 2 into the pure solution of type 1 until *mixing* occurs. (By this we mean the incorporation of type 2 chains into micelles of type 1.) Equations 8 and 9 and similar ones for type 2 are used to determine the two end points of the comicellization boundary, where displacement of one type of chain, making up the monodisperse micelles, by the other occurs. This in principle also determines the maximum chemical potential attainable for each species. To determine how p_1 and p_2 vary along the comicellization boundary, we use eq 7, and we use eqs

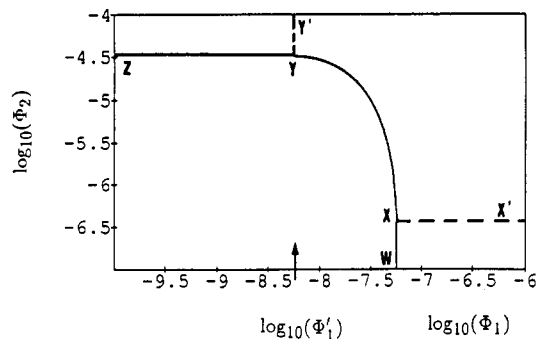


Figure 2. Plot of $\log \Phi_2$ versus $\log \Phi_1$ for $\chi_{AB} = 0$ showing the comicellization boundary XY , micellization boundaries WX and YZ , and the mixing lines XX' and YY' .

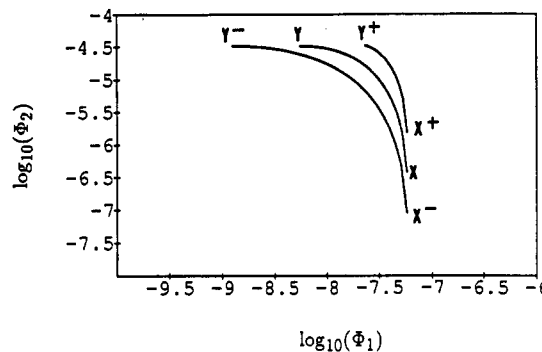


Figure 3. Effect of varying the interaction parameter χ_{AB} on the comicellization boundary. X^-Y^- , XY , and X^+Y^+ are for $\chi_{AB} = -0.1, 0$, and $+0.1$ respectively.

5 and 6 to determine Φ_1^{ccc} and Φ_2^{ccc} . The evolution of p_1 and p_2 depends on the physical and chemical characteristics of the two type of chains. In the next section we present case studies for certain types of chains with different interaction parameters χ_{AB} .

II.2. Phase Diagram. Experimentally the simplest control variables are Φ_1 and Φ_2 , the volume fractions of the two species of diblock copolymers. Some typical results are summarized in Figures 2 and 3 in the form of a phase diagram. These figures are for specific values of N , N_1 , N_2 , and γ_{eff} ; broadly similar results are obtained for a wide range of these parameters. Figure 2 is for $\chi_{AB} = 0$ and in Figure 3 we show the effect of varying the interaction parameter χ_{AB} on the comicellization boundary. We discuss them in turn.

Case 1: $\chi_{AB} = 0$. It is instructive to consider first the case when the entire core is made of the same species ($A = B$). By setting $\chi_{AB} = 0$, i.e., $F_{\text{core}} = 0$ in eq 1, we see that for comicellization to occur, we require $\Delta\mu > 0$ as one of the conditions.

The phase diagram of Figure 2 was calculated numerically from eqs 5–7, where the following physical and chemical parameters were used: $N = 15$, $N_1 = 500$, $N_2 = 4000$, and $\gamma_{\text{eff}} = 8$. With these parameters we find, $\Phi_1^{\text{cmc}} = 5.87 \times 10^{-8}$, $p_1^{\text{cmc}} = 26.4$, $\Phi_2^{\text{cmc}} = 3.26 \times 10^{-5}$, and $p_2^{\text{cmc}} = 14.7$. The solid lines WX and YZ represent the micellization boundaries while XY is the comicellization boundary. The dashed lines XX' and YY' represent the mixing lines.

For the above parameters we find from eq 7 the total number of chains making up the comicelle to decrease monotonically from $p = p_1^{\text{cmc}}$ to $p = p_2^{\text{cmc}}$ along the comicellization boundary in the direction X to Y . It can be shown perturbatively that in general $\delta p = -(\delta c_2)^3$ for small departures away from X along the comicellization boundary. In our example p_1 decreases monotonically

from p_1^{cmc} at X to 0 at Y . This allows us to predict Φ'_1 , the value of Φ_1 at Y , via eq 6 by setting $p_2 = p_2^{\text{cmc}}$ and $\Phi_2 = \Phi_2^{\text{cmc}}$. This reduces eq 6 to

$$(\Delta\mu)' = \left[\frac{9}{10} \log \left(\frac{N_2}{N_1} \right) + \frac{1}{5} \left(\frac{\Delta N}{N_2} \right) \right] (p_2^{\text{cmc}})^{1/2} \quad (10)$$

and Φ'_1 follows.

Referring to Figure 2, we may predict the effects of increasing the volume fractions of both species at fixed ratio $K = \Phi_2/\Phi_1$. Suppose we start with unassociated chains of both types 1 and 2 in a ratio such that $K < (N_2/N_1)^{2/5}$. This is obtained by setting $\Delta\mu < 0$. Increasing the volume fractions at fixed K causes the shorter of the two species to micellize when $\Phi_1 = \Phi_1^{\text{cmc}}$, i.e., upon crossing the micellization boundary WX . The addition of more materials leads to the incorporation of free long chains so as to form comicelles upon crossing the mixing line XX' (which corresponds to $\Phi_2 = \Phi_1^{\text{cmc}}(N_2/N_1)^{2/5}$). Similarly for $K > (\Phi_2^{\text{cmc}}/\Phi'_1)$ we pass through regions of free chains, monodisperse long micelles with free chains, and then comicelles with free chains. For intermediate K , $(N_2/N_1)^{2/5} < K < (\Phi_2^{\text{cmc}}/\Phi'_1)$, we cross only the comicellization boundary XY , and the system jumps from a state of unaggregated species directly to comicelles (containing comparable p_1, p_2) coexisting with free chains.

In a monodisperse solution of diblock copolymer, the driving force to micellization is the reduction in the high surface energy of the molten head blocks, which overcomes the loss of translational entropy, and the increased excluded-volume energy from the corona layer. The same driving force that micellizes pure species will also comicellize mixed species. We can qualitatively explain what happens at the two ends of the comicellization boundary. In the situation where we started initially with small micelles, the addition of a longer chain into the micelle decreases the inner corona energy since the addition is normally associated with the ejection of shorter chains from the micelle. Hence this counteracts the loss of translational entropy of the long chains. The gain in the outer corona energy is counteracted by the loss in effective surface energy of the B heads of the diblock, which leads to a net lowering in the free energy. In the other case, where we started with pure long micelles, the ejection of a single long chain is associated with the addition of more than one short chains. The increase in the inner corona energy is counteracted by the decrease in outer corona energy and the loss of interfacial energy of the short chains resulting again in a net lowering of the free energy. The interplay among these factors determines how the comicelles evolve along the comicellization boundary.

Case 2: $\chi_{AB} < 0$. We adopt the same procedures as above to determine the comicellization chemical potentials of the two species via eqs 5 and 6.

In this case there is mutual attraction between the two insoluble blocks of the diblock copolymers, causing a further lowering in the free energy of the comicelle on comicellization in addition to that caused by the reduction in the interfacial energy. A study of eq 1 reveals that comicellization can now occur for $\Delta\mu < 0$.

Using all the above parameters but setting $\chi_{AB} = -0.1$ we perform similar calculations and summarize our results in Figure 3. Figure 3 shows the effect of varying the interaction parameter on the comicellization boundary XY . We find that with χ_{AB} negative, the comicellization boundary now extends over a wider range of Φ_1 and Φ_2 . This of course means that the range over which monodisperse micelles can form in coexistence with free chains becomes narrower. For this particular value of χ_{AB} , p

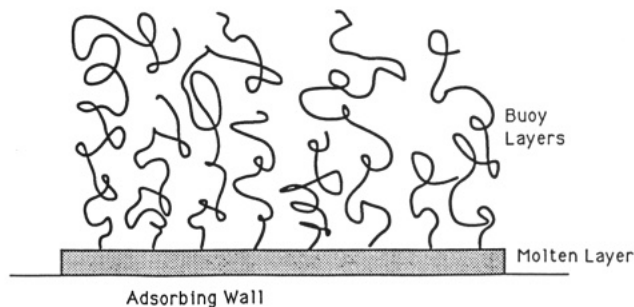


Figure 4. Bimodal brush on an attractive wall.

decreases monotonically from p_1^{cmc} to p_2^{cmc} as we traverse along the comicellization curve from X^- to Y^- , with p_2 increasing monotonically from 0 at X^- to p_2^{cmc} at Y^- .

Case 3: $\chi_{AB} > 0$. For slightly positive χ_{AB} we can still get comicellization between the two species, but the range over which this occurs is now very much reduced as can be seen from Figure 3. Provided that the effective surface energy is high, this still provides a lowering in the free energy of the comicelle despite the mutual repulsion of the two species in the core. We of course assume that the solvent is still expelled from the core. This approximation is valid provided the repulsion is of weak order compared to the interfacial energy, i.e., $\gamma_{\text{eff}} \gg \chi_{AB}N^{1/3}$. For greater incompatibility between the A and B blocks we may expect solvent to interpenetrate into the core, invalidating our initial assumptions.

Again for illustrative purposes we now set $\chi_{AB} = +0.1$. In Figure 3 we find the comicellization boundary now extends over a narrower range of Φ_1 and Φ_2 . We now find, as we traverse from X^+ to Y^+ along the comicellization boundary, p_2 to increase monotonically from 0 to about 13 at Y^+ (11% lower than p_2^{cmc}). There is also a finite jump in p_1 at Y^+ of about 5.4. This finite jump in p_1 provides a greater reduction in surface energy to counteract the repulsive interaction of the bimodal core species; qualitatively one can distinguish this first-order transition on crossing the mixing line from the second-order behavior, in which p_1 goes smoothly to zero, described above. However, we should note that the behavior will always be continuous when entropy of mixing effects are included (see section II.1).

We have found numerically that first-order behavior at the mixing line YY' can occur even for $\chi_{AB} = 0$ if the molecular weight of the longer chain is increased substantially from that used above. The same behavior is not, however, found along the XX' line for any reasonable parameter values.

III. Coadsorption at an Impenetrable Wall

We now address the problem of competitive adsorption onto an impenetrable wall (see Figure 4) and determine the concentrations and conditions required for coadsorption to occur. We again assume that A and B have the same interfacial properties with the solvent and the wall but not with each other. In the presence of a wall W attractive to the blocks A and B, the system may lower its free energy by adsorbing to the wall. We assume complete wetting, that is to say the entire surface is covered with the anchor blocks. The precipitation of the insoluble blocks onto the wall reduces the molten core surface energy of the diblock in solution, but by adsorbing onto the wall it pays the penalty for loss of translational entropy and increase in excluded-volume interaction of the C blocks, which are also stretched away from the wall. The balance of these factors determines whether the diblock copolymer

will precipitate onto the surface or not. With a bimodal distribution of diblock copolymers, we find that a bimodal brush may form for $\Phi_1 < \Phi_1^{\text{cac}}$ and $\Phi_2 < \Phi_2^{\text{cac}}$ (cac, critical adsorption concentration).¹ In other words, a mixed brush may arise in a concentration regime where neither of the species would adsorb in the absence of the other.

Using again the model of Marques et al.¹ and following analogous steps to those given above for the comicellization case, we construct the grand canonical free energy Ω per unit area of surface, which has the following form:

$$\Omega(\sigma, \sigma_2) \sim -S + c/\sigma^2 + N_1\sigma^{11/6} + (N_2 - N_1)\sigma_2^{11/6} + \chi_{AB}N(\sigma - \sigma_2)\sigma_2/\sigma - \mu_1\sigma - \Delta\mu\sigma_2 \quad (11)$$

where S is the spreading power¹⁸ defined as $S = \gamma_{\text{WO}} - \gamma_{\text{AO}} - \gamma_{\text{WA}} = \gamma_{\text{WO}} - \gamma_{\text{BO}} - \gamma_{\text{WB}}$. We consider the case when $S > 0$, which tends to flatten the molten A and B anchor layer. The term c/σ^2 is the van der Waals contribution to the molten layer with $c = H/12\pi N^2$, H being the modulus of the negative Hamaker constant, which has the effect of thickening the layer. The next two terms are the so-called buoy energy formed by the C blocks calculated in a scaling "blob" description.¹² The inner and the other buoy size of order $N_1\sigma^{1/3}$ and $\Delta N\sigma_2^{1/3}$, respectively. The term in χ_{AB} is the mean-field result for the interaction of the two core species. The μ 's are the usual chemical potentials of the two species. As in the comicellization case, we ignore the entropy of mixing of type 1 and 2 chains within the layer; these yield exponentially small corrections to the partial coverages whenever the model, treated here, predicts the formation of a monodisperse brush of a single species. These entropy terms also yield corrections when both partial coverages (σ_1, σ_2) are very small—a regime in which the scaling description of the brush, on which our model is based, ceases to be valid. In principle eq 11 is valid for $\sigma_1, \sigma_2 > (H/4\pi SN^2)^{1/2}$; at lower coverages the van der Waals term is inaccurate.¹

Minimization of Ω , eq 11, with respect to σ and σ_2 leads respectively to equations for the chemical potentials

$$\mu_1(\sigma, \sigma_2) = -2c/\sigma^3 + (11/6)N_1\sigma^{5/6} + \chi_{AB}N\sigma_2^2/\sigma^2 \quad (12)$$

and

$$\Delta\mu(\sigma, \sigma_2) = (11/6)(N_2 - N_1)\sigma_2^{5/6} + \chi_{AB}N(1 - 2\sigma_2/\sigma) \quad (13)$$

To find the onset of adsorption of one or both of the two species, we set $\Omega \simeq 0$ to give

$$3c/\sigma^2 - (5/6)N_1\sigma^{11/6} = S + (5/6)(N_2 - N_1)\sigma_2^{11/6} \quad (14)$$

after eliminating μ_1 and $\Delta\mu$ using eqs 12 and 13.

We adopt the same procedures as used in section II for the comicellization case to determine the chemical potentials required for adsorption and coadsorption. We again fix $K = \Phi_2/\Phi_1$ and start at concentrations such that $\Phi_1 < \Phi_1^{\text{cac}}$ and $\Phi_2 < \Phi_2^{\text{cac}}$. We keep adding more types 1 and 2 until either adsorption or coadsorption onto the wall occurs. Alternatively we can fix $\Phi_1 < \Phi_1^{\text{cac}}$ and imagine adding type 2 chains until both species or one of the species adsorbs onto the wall. Therefore for a given Φ_1 , eqs 12 and 14 determine σ and σ_2 at the minimum of $\Omega(\sigma, \sigma_2)$ at coadsorption. Equation 13 is used to calculate the amount of type 2 required in solution for coadsorption. The two concentrations at which coadsorption takes place are referred to as critical coadsorption concentrations (ccac). The locus of these points on the phase diagram defines the coadsorption boundary. As before we define the mixing lines across which the character of the adsorbed layer changes from a single species to a mixed brush.

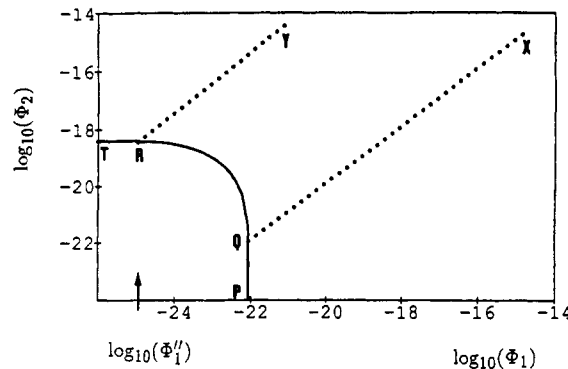


Figure 5. Plot of $\log \Phi_2$ versus $\log \Phi_1$ for $\chi_{AB} = 0$ showing the coadsorption boundary QR , adsorption boundaries PQ and RT , and the mixing lines QX and RY .

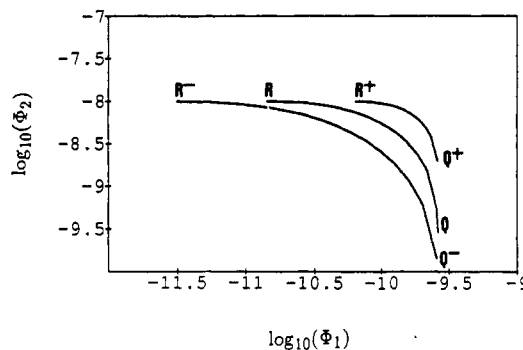


Figure 6. Effect of varying the interaction parameter χ_{AB} on the adsorption boundary. Q^-R^- , QR , and Q^+R^+ are for $\chi_{AB} = -0.1, 0$, and $+0.1$, respectively.

Phase Diagram. We consider the case when both $\Phi_1^{\text{cac}} < \Phi_1^{\text{cmc}}$ and $\Phi_2^{\text{cac}} < \Phi_2^{\text{cmc}}$; i.e., both pure species in solution will adsorb onto the wall well before the critical concentration for micellization is attained.

The equilibrium coverage σ_i^{cac} at which critical adsorption occurs for each of the pure species i in solution is given by solving the equation

$$S - 3c/\sigma_i^2 + (5/6)N_i\sigma_i^{11/6} = 0 \quad (15)$$

and the critical chemical potential is given by

$$\mu_i^{\text{cac}} = -2c/(\sigma_i^{\text{cac}})^3 + (11/6)N_i(\sigma_i^{\text{cac}})^{5/6} \quad (16)$$

As before we consider three cases where χ_{AB} is zero, negative, and slightly positive. Typical results are summarized on phase diagrams in Figures 5 and 6. To see coadsorption over a reasonable range of volume fractions, it is necessary for the C blocks of the two chains to be quite close in length. This condition results from the linear N dependence in the second term on the right in eq 16, which contrasts with the weak logarithmic dependence found earlier for the comicelles.

As an illustrative example we use the following parameters for our case studies: $N = 15$, $N_1 = 400$, $N_2 = 450$, $S = 1$, $H = 10$, and $\gamma_{\text{eff}} = 8$. With these parameters we get $\sigma_1^{\text{cac}} = 0.04206$, $\Phi_1^{\text{cac}} = 2.61 \times 10^{-10}$, $\Phi_1^{\text{cmc}} = 3.93 \times 10^{-7}$, $\sigma_2^{\text{cac}} = 0.04120$, $\Phi_2^{\text{cac}} = 1.01 \times 10^{-8}$, and $\Phi_2^{\text{cmc}} = 6.43 \times 10^{-7}$. Figure 5 is a phase diagram for $\chi_{AB} = 0$. The solid lines PQ and RT are the adsorption boundaries separating regimes of a depleted wall from a monodisperse adsorbed brush, and QR is the coadsorption boundary separating a depleted wall from a bimodal brush. The dotted lines QX and RY are the mixing lines separating regimes of monodisperse brush and bimodal brush. With the above parameters we find as we traverse the coadsorption boundary from Q to R that σ , the total coverage, remains

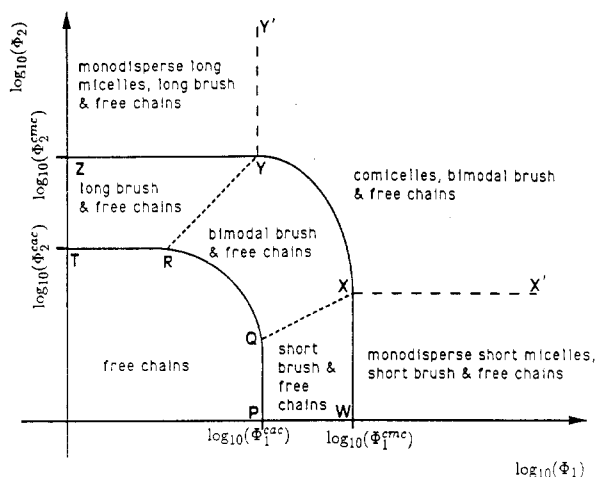


Figure 7. Schematic phase diagram showing the different regimes of adsorption, coadsorption, micellization, and comicellization.

almost constant while the ratio σ_1/σ varies smoothly from 1 to 0. The evolution path taken by σ_1 and σ_2 allows us to predict Φ_1'' , the value of Φ_1 at R, for which the brush at the wall becomes a monodisperse long brush. An estimate for Φ_1'' is given from eq 12 via $\mu_1'' = -2c/(\sigma_2^{cac})^3 + (11/6)N_1(\sigma_2^{cac})^{5/6}$.

Unlike micellization where the chemical potentials remain constant at μ_i^{cmc} for $\Phi_i > \Phi_i^{cmc}$, the chemical potential for the adsorption case can continue to increase on addition of more chains. Hence the mixing lines QX and RY, in the coadsorption case, are not parallel to the axes in the plot of Figure 5. Within our approximations μ_1 and μ_2 continue to increase logarithmically with Φ_1 and Φ_2 until micellization occurs. At this point the corresponding partial coverage ceases to increase further.

In Figure 6 we show the effect of varying the interaction parameter χ_{AB} on the coadsorption boundary. Like the comicellization case, the effect of increasing (decreasing) the incompatibility between the anchor species A and B reduces (increases) the range of the mixing ratio $K = \Phi_2/\Phi_1$ within which coadsorption occurs.

IV. Discussion and Summary

Although the model used above is rather crude, it provides a useful illustration of competitive adsorption and comicellization phenomena in block copolymers at the lower end of dilute bulk volume fractions of the species. With increasing concentrations of the species we need to take into account the bimodal distribution on the formation of stable mesophases such as lamellar bilayers, cylindrical phases, etc. We have also not addressed the interesting question of kinetics of exchange between the two species on comicellization. The problem of a bimodal distribution offers an interesting starting point for considering the more challenging case of a continuous distribution of chain length in the bulk.

Several variations to the problem addressed in this paper may be contemplated. For instance we have not considered

the case of a swollen core where the solvent is able to penetrate into the core. Also different core lengths of the two species may be considered. There is also the interesting case where one of the previously insoluble blocks is now in a good solvent but has a negative interaction χ parameter with the other insoluble block. In that case we can envisage the comicelles as consisting of the molten core of insoluble blocks coated by the block that has affinity for both the insoluble block and the solvent; the corona fanning from the core arises from both species of diblock copolymers. These phenomena are obviously complicated, but their further investigation may be warranted if suitable experiments become available.

In Figure 7 we summarize the results of this paper in a phase diagram that shows schematically where the different phenomena may arise. We assume that $\Phi_i^{cac} < \Phi_i^{cmc}$. Depending on the path taken through the phase diagram, one may on increasing the volume fractions of chains undergo various different sequences of adsorption, competitive adsorption, micellization, or comicellization. The general structure of this phase diagram should not depend too much on the chemical species involved, although as we have seen the actual values of the critical volume fractions depend sensitively on parameters such as chain length.

Acknowledgment. We thank Jason Brooks, Matthew Turner, and Pete Barker for helpful discussions. D.F.K.S. gratefully acknowledges financial support from Trinity College, Cambridge. This work was funded in part under EC Grant SC1-0288-C.

References and Notes

- (1) Marques, C.; Joanny, J. F.; Leibler, L. *Macromolecules* **1988**, *21*, 1051.
- (2) Leibler, L.; Orland, H.; Wheeler, J. C. *J. Chem. Phys.* **1983**, *79* (7), 3550.
- (3) Daoud, M.; Cotton, J. P. *J. Phys. Fr.* **1982**, *43*, 531.
- (4) Halperin, A. *J. Phys. Fr.* **1988**, *49*, 131.
- (5) Birshtein, T. M.; Zhulina, E. B. *Polymer* **1989**, *30*, 170.
- (6) Munch, M. R.; Gast, A. P. *Macromolecules* **1988**, *21*, 1360.
- (7) Halperin, A. *Macromolecules* **1987**, *20*, 2943.
- (8) Bug, A. L. R.; Cates, M. E.; Safran, S. A.; Witten, T. A. *J. Chem. Phys.* **1987**, *87* (3), 1824.
- (9) Semenov, A. N. *Sov. Phys.-JETP* **1985**, *61*, 733; *Zh. Eksp. Teor. Fiz.* **1985**, *88*, 1424.
- (10) See references cited in refs 2, 5, and 7 for examples.
- (11) Russel, W. B.; Saville, D. A.; Schowalter, W. R. *Colloidal Dispersion*; Cambridge University Press: Cambridge, 1989. Sonntag, H.; Streng, K. *Coagulation Kinetics and Structure Formation*; Plenum Press: New York and London, 1987.
- (12) de Gennes, P.-G. *J. Phys. (Les Ulis, Fr.)* **1976**, *37*, 1443. de Gennes, P.-G. *Macromolecules* **1980**, *13*, 1069.
- (13) Milner, S. T.; Witten, T. A.; Cates, M. E. *Macromolecules* **1988**, *21*, 2610.
- (14) Milner, S. T.; Witten, T. A.; Cates, M. E. *Macromolecules* **1989**, *22*, 853.
- (15) Munch, M. R.; Gast, A. P. *Macromolecules* **1988**, *21*, 1366.
- (16) Whitmore, M. D.; Noolandi, J. *Macromolecules* **1990**, *23*, 3321.
- (17) Ligoure, C.; Leibler, L. *J. Phys. Fr.* **1990**, *51*, 1313.
- (18) Shim, D. F. K.; Cates, M. E. *J. Phys. Fr.* **1989**, *50*, 3535.
- (19) Shim, D. F. K.; Cates, M. E. *J. Phys. Fr.* **1990**, *51*, 701.
- (20) Rowlinson, J. S.; Widom, B. *Molecular Theory of Capillarity*; Clarendon Press: Oxford, 1982.